ARTICLE

www.the-innovation.org

Unveiling a novel entry gate: Insect foregut as an alternative infection route for fungal entomopathogens

Yiling Lai,[1,2,4] Weilu Zheng,[1,2,4] Yitong Zheng,[1,2,4] Haiquan Lu,[1,3,4] Shuang Qu,[1] Lili Wang,[1,2] Muwang Li,[3] and Sibao Wang[1,2,*]
*Correspondence: sbwang@cemps.ac.cn

Received: April 10, 2024; Accepted: May 19, 2024; Published Online: May 22, 2024; https://doi.org/10.1016/j.xinn.2024.100644

GRAPHICAL ABSTRACT

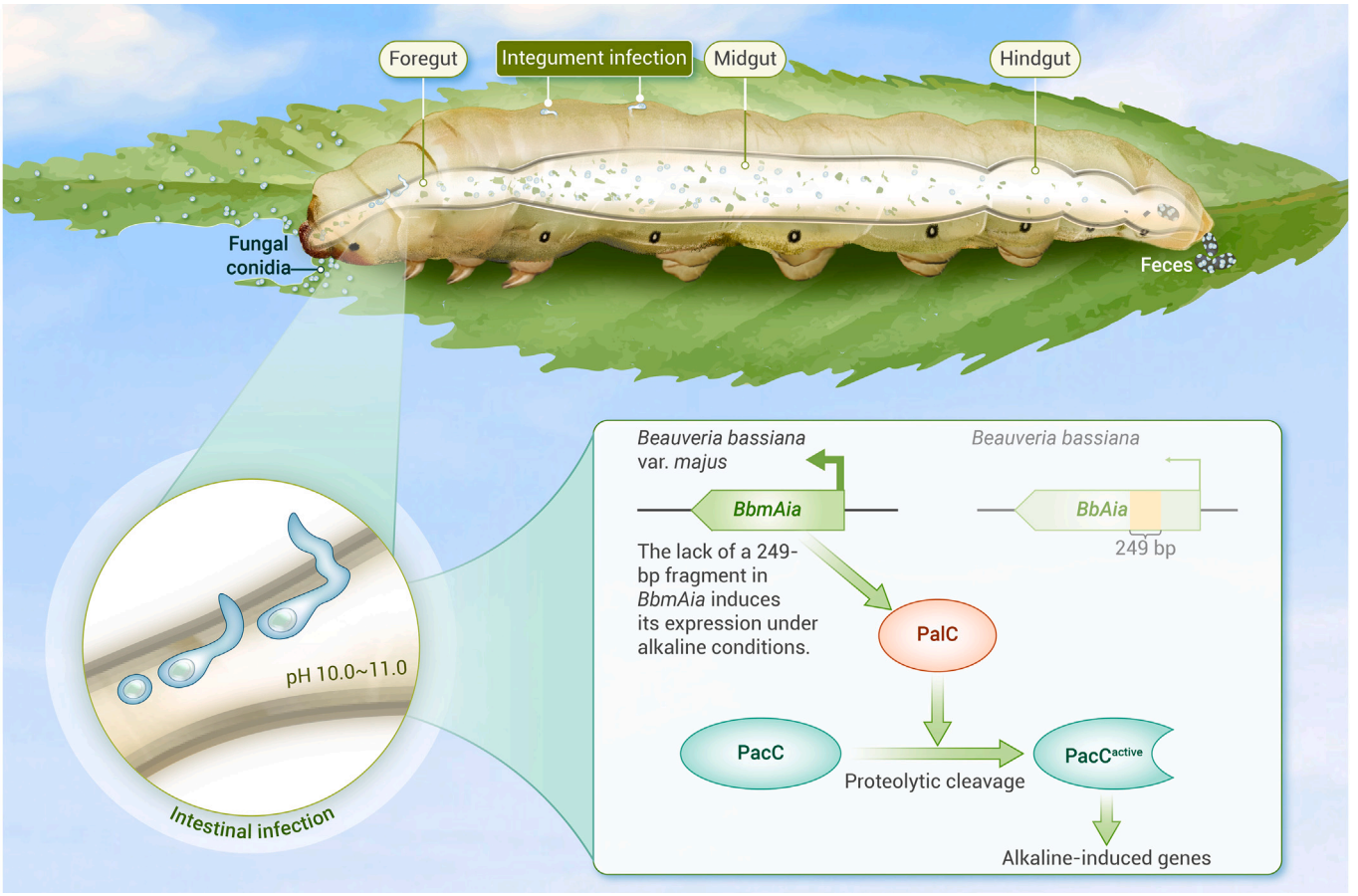

PUBLIC SUMMARY

- *Beauveria bassiana* var. *majus* (Bbm) can infect lepidopteran larvae through both the integument and gut.
- The insect foregut is discovered as a previously unrecognized route for fungal invasion.
- Bbm has evolved alkaline tolerance via a novel pH-responsive Aia-PalC-PacC cascade to colonize the hostile foregut.
- Aia in Bbm loses a 249-bp fragment, resulting in enhanced expression under alkaline conditions, which promotes *PalC* upregulation and PacC activation.

ARTICLE

The Innovation

Unveiling a novel entry gate: Insect foregut as an alternative infection route for fungal entomopathogens

Yiling Lai,[1,2,4] Weilu Zheng,[1,2,4] Yitong Zheng,[1,2,4] Haiquan Lu,[1,3,4] Shuang Qu,[1] Lili Wang,[1,2] Muwang Li,[3] and Sibao Wang[1,2,*]

[1]New Cornerstone Science Laboratory, CAS Key Laboratory of Insect Developmental and Evolutionary Biology, CAS Center for Excellence in Molecular Plant Sciences, Chinese Academy of Sciences (CAS), Shanghai 200032, China

[2]CAS Center for Excellence in Biotic Interactions, University of Chinese Academy of Sciences, Beijing 100049, China

[3]Sericultural Research Institute, Jiangsu University of Science and Technology, Zhenjiang 212000, China

[4]These authors contributed equally

*Correspondence: sbwang@cemps.ac.cn

Received: April 10, 2024; Accepted: May 19, 2024; Published Online: May 22, 2024; https://doi.org/10.1016/j.xinn.2024.100644

Citation: Lai Y., Zheng W., Zheng Y., et al., (2024). Unveiling a novel entry gate: Insect foregut as an alternative infection route for fungal entomopathogens. The Innovation **5(4)**, 100644.

Insects and their natural microbial pathogens are intertwined in constant arms races, with pathogens continually seeking entry into susceptible hosts through distinct routes. Entomopathogenic fungi are primarily believed to infect host insects through external cuticle penetration. Here, we report a new variety, *Beauveria bassiana* var. *majus* (Bbm), that can infect insects through the previously unrecognized foregut. Dual routes of infection significantly accelerate insect mortality. The pH-responsive transcription factor PacC in Bbm exhibits rapid upregulation and efficient proteolytic processing via PalC for alkaline adaptation in the foregut. Expression of *PalC* is regulated by the adjacent downstream gene *Aia*. Compared to non-enteropathogenic strains such as ARSEF252, *Aia* in Bbm lacks a 249-bp fragment, resulting in its enhanced alkaline-induced expression. This induction promotes *PalC* upregulation and facilitates PacC activation. Expressing the active form of BbmPacC in ARSEF252 enables intestinal infection. This study uncovers the pH-responsive Aia-PalC-PacC cascade enhancing fungal alkaline tolerance for intestinal infection, laying the foundation for developing a new generation of fungal insecticides to control destructive insect pests.

INTRODUCTION

Insects, Earth's most diverse and abundant creatures, have long played host to a range of pathogens like viruses, bacteria, and fungi. Among these entomopathogens, fungi dominate as the primary cause of insect diseases. Notably, entomopathogenic fungi form the largest group of insect pathogens, playing a vital role in regulating insect populations in ecosystems.[1,2] In tackling the challenges of insecticide resistance, fungal pesticides, particularly those belonging to the genera *Beauveria* and *Metarhizium*, have been developed as eco-friendly and sustainable biocontrol agents against agricultural insect pests and vectors of human diseases.[3–5]

Insect hosts and their natural microbial pathogens are intertwined in a constant arms race.[6–8] This tight interaction involves the constant attempt of pathogens to gain access to susceptible insect hosts through distinct routes. Unlike other entomopathogens such as bacteria, viruses, protists, and microsporidia, which infect their insect hosts through the midgut, entomopathogenic fungi are traditionally thought to invade insects by penetrating the integument.[9] Yet, the effectiveness of topically applied fungal insecticides is influenced by various adverse environmental factors, including solar ultraviolet light, extreme ambient temperature, and low humidity, which can impede fungal conidial germination on the external cuticle.[10,11] Fungal conidia can only germinate on the insect's external cuticle under favorable temperature and humidity conditions.[12,13] Therefore, the pursuit of alternative routes for fungal infection, such as via the insect gut, emerges as a strategic endeavor to surmount the challenges posed by ambient abiotic factors.[14] However, the insect gut, characterized by an unfavorable pH, teeming microbiota, and swift food passage, presents an antagonistic realm for fungal survival and propagation.[15] The inhibitory impact of high alkalinity on fungal conidial germination within the larval gut of *Bombyx mori* (Lepidoptera: Bombycidae) and *Heliothis zea* (Lepidoptera: Noctuidae) underscores this formidable environment.[16,17] Moreover, gut-residing bacteria in locusts unleash antifungal compounds that inhibit fungal conidial germination.[18] Despite efforts since the 1930s to identify fungal strains capable of infecting insects through the intestinal tract,[15,19–22] convincing evidence with explicit histological information to support fungal gut infection has been lacking.[19]

In this study, we have identified a new variety of *Beauveria bassiana*, designated as *Beauveria bassiana* var. *majus* (Bbm), capable of infecting lepidopteran larvae through both the integument and the foregut. The dual routes of infection significantly accelerate the speed of lethality, offering a promising approach for the effective management of lepidopteran pests. Notably, Bbm strains invade the alkaline foregut of lepidopteran larvae through a novel pH-responsive pathway involving the Aia-PalC-PacC signaling cascade. Overall, our findings uncover the insect foregut as an alternative and previously unrecognized route of infection by entomopathogenic fungi. We have also identified that the pH-responsive Aia-PalC-PacC signaling cascade facilitates fungal tolerance to alkaline foreguts, thereby enabling intestinal infection. The discovery of Bbm, with enhanced infectivity through both the integument and the foregut, opens a promising way for improving the efficacy of fungal insecticides, leading to efficient and environmentally friendly pest control.

RESULTS

Invasion of intestinal tract by two *B. bassiana* strains

Previous studies showed that gut bacteria play a protective role against intestinal infection by the fungal pathogen *Metarhizium anisopliae* in locusts.[23] We initially attempted to investigate whether gut bacteria act as a protective barrier against invasion by *B. bassiana* in the larval gut of a lepidopteran model insect, silkworm *B. mori*.[24] We began our investigation by selecting a highly virulent strain of *B. bassiana* against silkworm larvae through insect bioassays. The virulence of 14 *B. bassiana* strains (Table S1) was evaluated by spraying a suspension of 5×10^7 conidia/mL onto the cuticle of fifth-instar day-2 *B mori* larvae. Recognizing that higher humidity favors conidial germination,[10,25] we initially maintained the inoculated larvae under high ambient humidity conditions (>96% relative humidity [RH]) for the first 48 h post-topical inoculation, followed by a regulated humidity environment at 80% ± 5% RH. Among the 14 *B. bassiana* strains studied, strain Bbm1, which was isolated from a silkworm larva cadaver, exhibited the highest virulence, with all larvae dying 3 days after Bbm1 topical inoculation (Figure 1A). In contrast, the ARSEF252 strain exhibited significantly lower virulence.

To investigate the potential role of gut commensal bacteria in preventing fungal intestinal infection, we eliminated gut bacteria of silkworm larvae by feeding them with antibiotics-sprayed fresh mulberry leaves, starting from the first day of the third instar until they underwent *per os* inoculation (Figure S1). Fifth-instar day-2 silkworm larvae were subsequently fed fresh mulberry leaves inoculated with the conidia of either Bbm1 or ARSEF252. The larvae were then reared under constant low ambient humidity conditions (35% ± 5% RH), wherein topically applied *B. bassiana* did not cause larval mortality (Figure S2), aiming to minimize the likelihood of cuticular infection. Surprisingly, *per os* administration of Bbm1 resulted in infections in both silkworm larvae without gut microbiota and untreated larvae with gut microbiota at comparable rates, indicating that the presence of the gut microflora had no obvious impact on *per os* infection by Bbm1. Conversely, the strain ARSEF252 failed to induce infection through the intestinal tract in silkworm larvae, irrespective of the presence or absence of gut microbiota (Figure 1B).

To validate the intestinal infection of silkworm larvae by Bbm1, we orally inoculated 1×10^5 conidia per larva using a 2-μL micropipettor (Figure 1C), followed by immediate surface sterilization and incubation under low humidity conditions (35% ± 5% RH). Out of the ten *B. bassiana* strains tested, only Bbm1

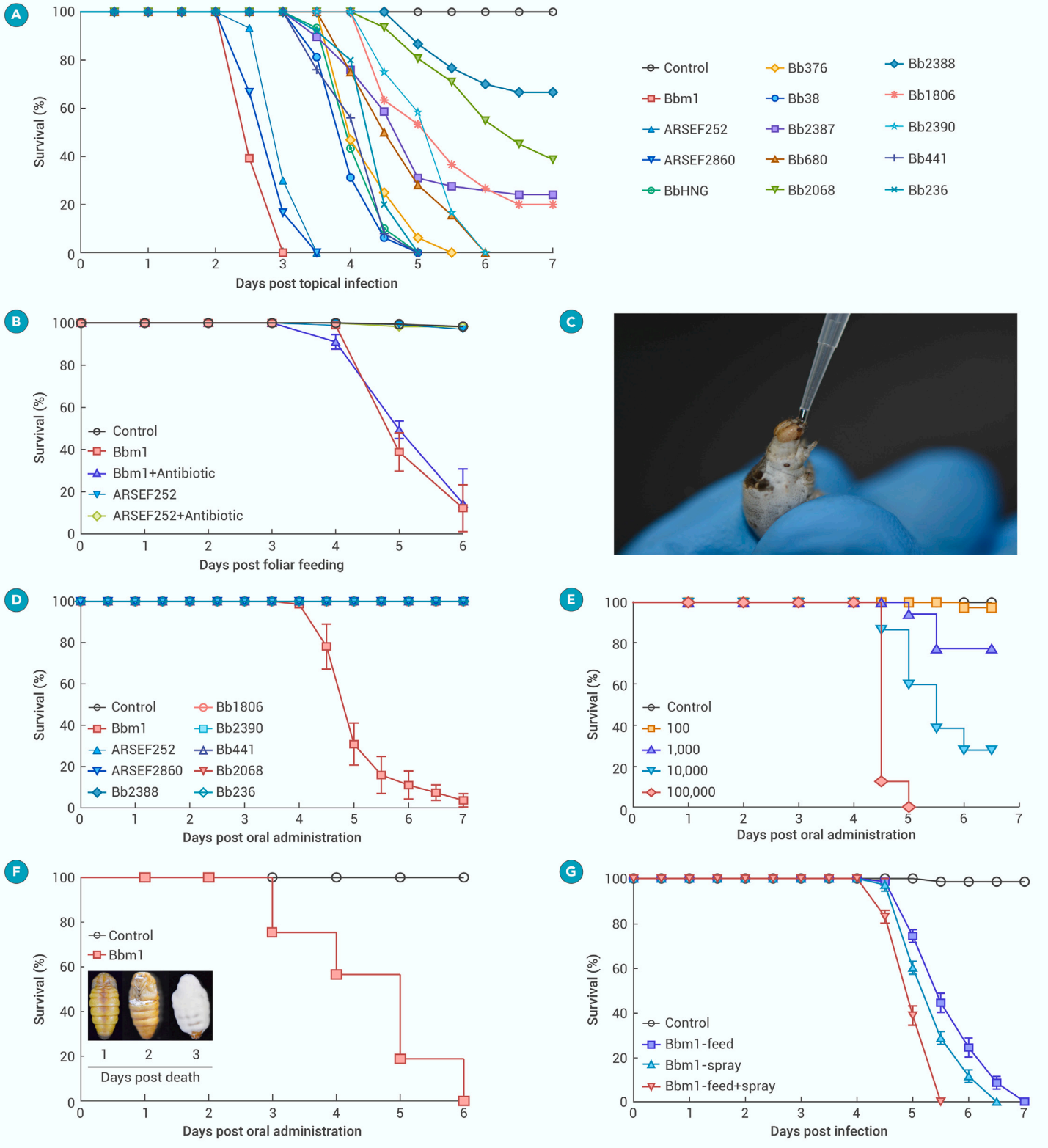

Figure 1. Screening for the high-virulent strains of *B. bassiana* and intestinal infection of *B. mori* larvae by Bbm1 (A) Survival of fifth-instar day-2 silkworm larvae following topical inoculation with a suspension of different *B. bassiana* strains containing 5 × 10^7 conidia/mL. Control insects were sprayed with 0.01% Triton X-100. (B) Effect of gut microbiota on intestinal infection of silkworm larvae treated with or without antibiotics by *B. bassiana* strains Bbm1 and ARSEF252. Fifth-instar day-2 larvae were inoculated *per os* by feeding with fresh mulberry leaves that had been dipped in conidia suspension (2 × 10^7 conidia/mL) followed by air drying and then were reared at 35% ± 5% RH. The error bars represent the mean ± SD. (C) Oral administration of *B. bassiana* conidia to a silkworm larva using a 2-μL micropipette. (D) Survival rate of conventionally reared silkworm fifth-instar day-2 larvae after *per os* inoculation with 1 μL conidia suspension (1 × 10^8 conidia/mL) of nine different *B. bassiana* strains using a 2-μL micropipette. The error bars represent the mean ± SD. (E) Survival rate of silkworm larvae after oral administration of different dosages (100, 1,000, 10,000, and 100,000 conidia/larva) of Bbm1 conidia. (F) Survival rate of older larvae after *per os* inoculation with Bbm1 (10^5 conidia/larva). The survival rate shown is one of three biological replicates with similar results. (G) Additive effect of dual routes of infection with Bbm1 on larval mortality after *per os* and topical inoculation. Fifth-instar day-2 larvae were inoculated by feeding mulberry leaves that had been sprayed with fungal conidia or by topical inoculation. The experiment was performed in three biological replicates. The error bars represent the mean ± SD.

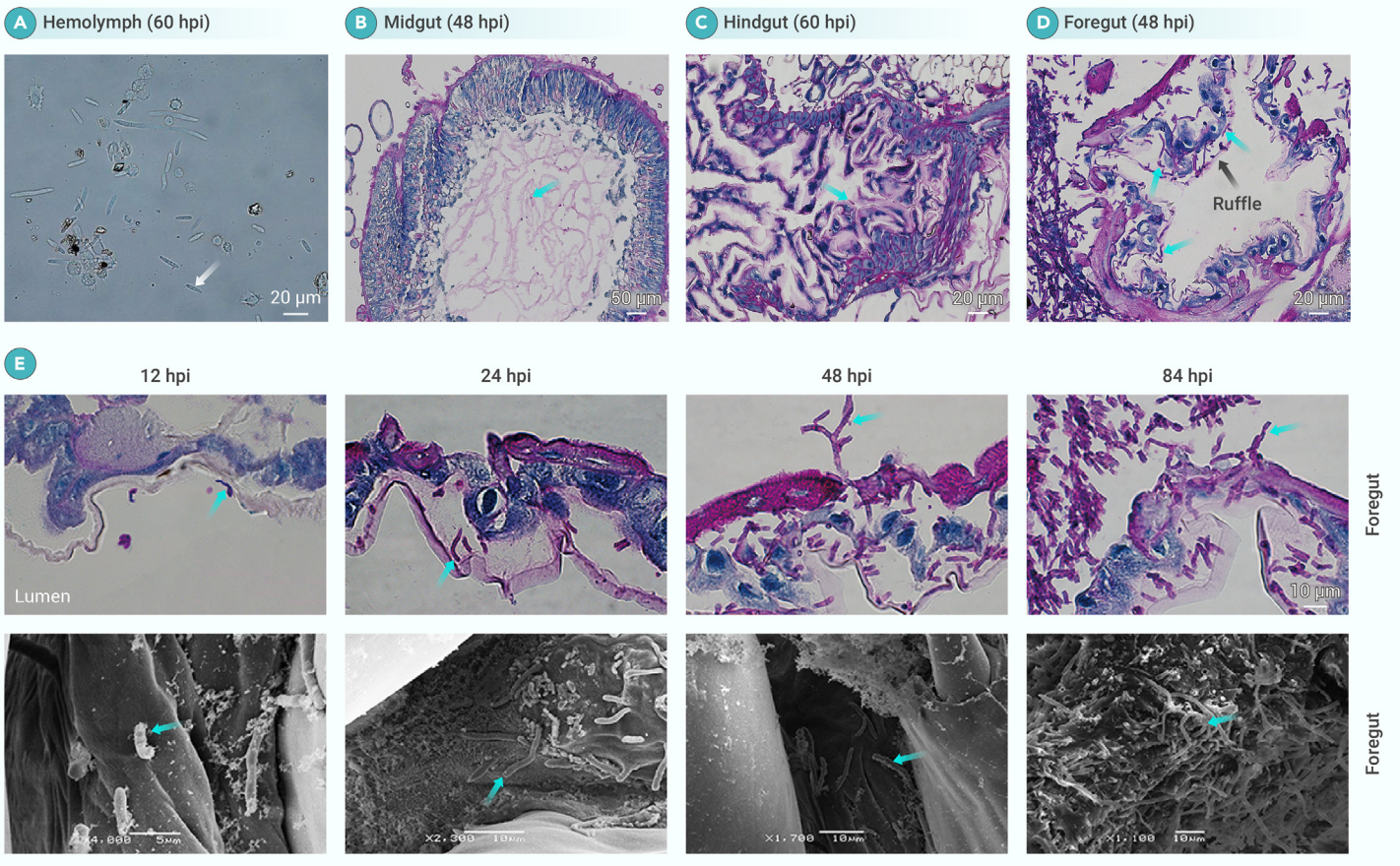

Figure 2. The foregut is the sole invasion site for *B. bassiana* Bbm1 within the intestinal tract (A) Hyphal bodies (white arrow) were detected in the larval hemolymph at 60 h after oral administration with Bbm1. (B and C) Light micrographs of Periodic Acid-Schiff (PAS)-stained semithin sections of the larval midgut (B) and hindgut (C) 48 h after oral administration of Bbm1. Note that germinated conidia of Bbm1 were not found in the lumen of the midguts or hindguts 48 h after oral administration. (D) Light micrographs of PAS-stained semithin sections of the larval foreguts at 48 h after oral administration of Bbm1, showing hyphae of *B. bassiana* Bbm1 penetrating the foregut wall. The foregut displays six ruffles (black arrow) along its intima. (E) Time course of larval infection. Top: light micrographs of PAS-stained semithin sections of larval foreguts obtained at 12, 24, 48, and 84 h after *per os* inoculation with *B. bassiana* Bbm1. Bottom: scanning electron micrographs of larval foreguts after *per os* inoculation with Bbm1 as on the top. The lake blue arrows indicate conidia or mycelia of *B. bassiana* Bbm1.

and Bbm2 could infect the larvae through *per os* inoculation (Figures 1D and S3). We then performed a dose-response curve for *per os* infectivity using fifth-instar silkworm larvae and found that an inoculum of 1×10^5 conidia per larva resulted in 100% mortality 5 days post-*per os* inoculation (Figure 1E). These results demonstrated that Bbm1 can infect the larvae via both the external cuticle and the intestinal tract.

Dual-route infection enhances *B. bassiana* Bbm's efficacy against older larvae

Older instar larvae and pupae are usually less susceptible to fungal topical infection.[26–28] To examine whether Bbm1 could infect older instar larvae through the gut, we administered *B. bassiana* Bbm1 *per os* to fifth-instar larvae on the last day before pupation. We observed that all the treated larvae died at the pupal stage 6 days after *per os* inoculation with Bbm1. The fungus first emerged from the anterior portion of the pupae and later covered the entire pupal cuticle (Figure 1F).

To assess the potential additive effect between *per os* and cuticular infection, we conducted dual-route infection of silkworm larvae by Bbm1. We found that simultaneous infection via both modes of inoculation significantly enhanced the killing speed against the larvae compared to either topical or *per os* inoculation alone ($p < 0.0001$, log-rank [Mantel-Cox] test) (Figure 1G). This result indicates that the addition of an alternative route of intestinal infection can augment the efficacy of fungal insecticides.

Clanis bilineata, a member of the Lepidopteran family *Sphingidae,* represents a major agricultural pest causing considerable damage to soybean production. Oral inoculation of *C. bilineata* larvae with 1 μL of Bbm1 conidia suspension containing 1×10^8 conidia/mL resulted in larval infection. The infected larvae showed typical symptoms of fungal infection, and the cadavers mummified and became mycosed after death (Figure S4).

The insect foregut serves as an alternative route for fungal invasion

Numerous hyphal bodies were observed in the hemolymph of silkworm larvae 60 h after *per os* inoculation with Bbm1 (Figure 2A). To determine the portal site of Bbm1 invasion within the larval gut, we employed histology to examine the larval midgut, the primary invasion site for entomopathogenic bacteria, viruses, and parasites, at 48 h after *per os* inoculation with Bbm1. Although a few conidia were observed in the midguts of *per-os*-inoculated larvae, no hyphal growth and penetration of the midgut wall was observed, indicating that the midgut is not the invasion site of Bbm1 (Figure 2B). The same observation was made for the hindgut (Figure 2C). Unexpectedly, numerous penetrating fungal hyphae were found in the foregut. Forty-eight hours after *per os* inoculation, many hyphae of Bbm1 had crossed the foregut wall and translocated to the hemocoel (Figure 2D). In contrast, no hyphae were observed in the foregut of larvae even at 60 h after topical inoculation (Figure S5). To monitor the time course of infection, we dissected larval guts (foregut, midgut, and hindgut) at 12, 24, 48, and 84 h after oral inoculation with 1 μL of 1×10^8 conidia/mL. We then examined the guts for the presence of conidia and hyphae (Figure 2E). By 12 h after feeding, the fungal conidia had germinated to form germ tubes in the foregut. By 24 h post-inoculation, the hyphae had penetrated the foregut epithelia. Many hyphae were observed in the foregut 48 h after *per os* inoculation (Figure 2E). In contrast, no germinated conidia were detected in the midguts or hindguts of the inoculated larvae (Figure S6). Similarly, conidial germination and hyphal penetration of the gut tissues (foregut, midgut, or hindgut) were not observed in any ARSEF252 conidia-fed larvae

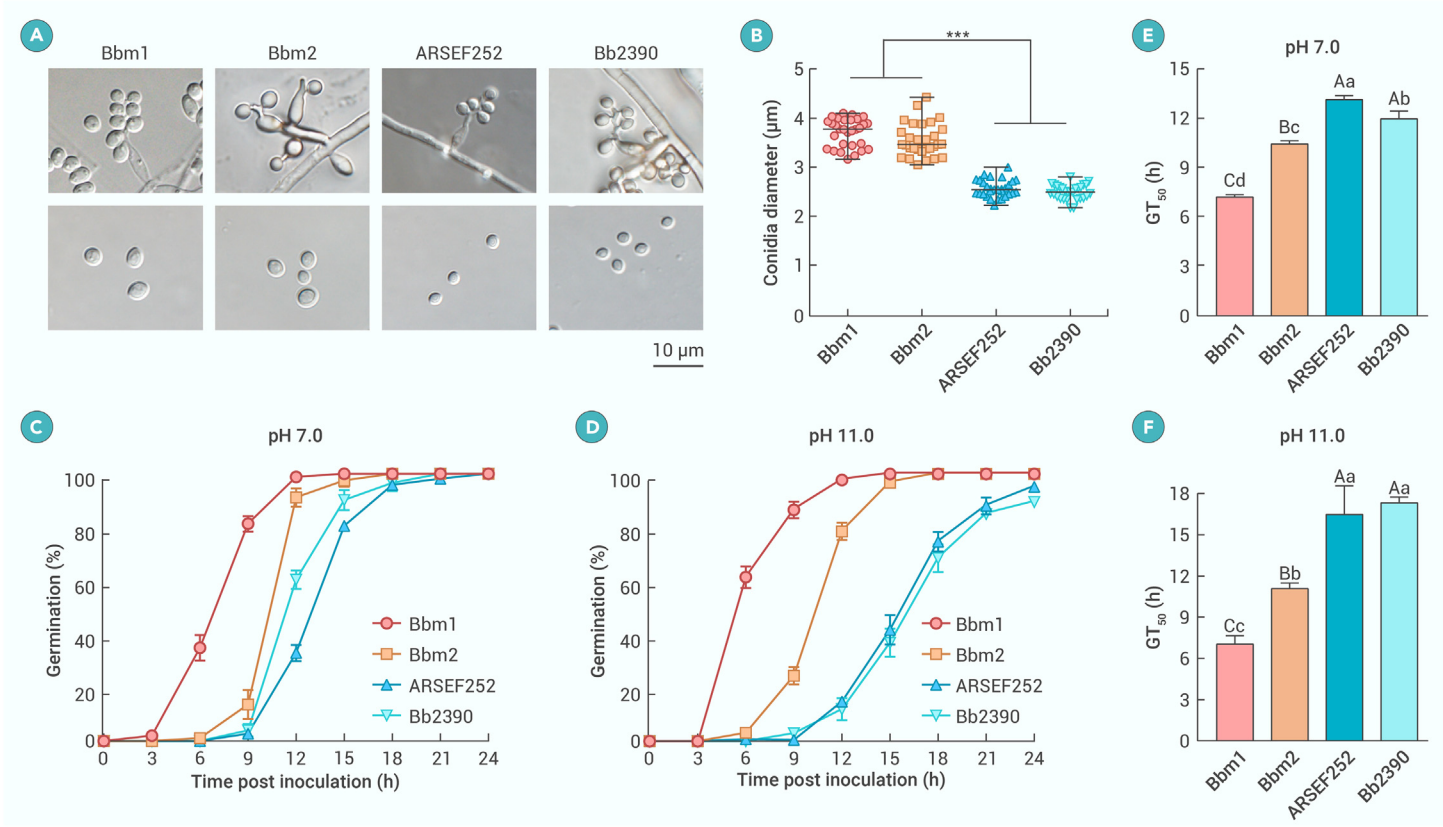

Figure 3. *B. bassiana* conidia and effect of pH on conidial germination of the *B. bassiana* strains (A) Conidiogenous cells and conidia of *B. bassiana* strains. (B) Conidia (n = 30) diameter of *B. bassiana* strains. The error bars represent median with range. ***$p < 0.001$. (C and D) Germination rate of Bbm1, Bbm2, ARSEF252, and Bb2390 after culture in SDB liquid medium at pH 7.0 (C) and 11.0 (D). The error bars represent the mean ± SD. (E and F) Median germination time (GT_{50}) of Bbm1, Bbm2, ARSEF252, and Bb2390 conidia at pH 7.0 (E) and 11.0 (F). Experiments were performed in three biological replicates. The error bars represent the mean ± SD. Capital letters, $p < 0.01$; lowercase letters, $p < 0.05$.

(Figure S7). These results indicate that the foregut is the sole intestinal invasion site for Bbm1.

Bbm conidia exhibit rapid germination

The strains Bbm1 and Bbm2 were originally isolated from silkworm cadavers in Jingxian (Anhui Province, China) and Xincheng (Guangxi Province, China), respectively (Figure S8A). Fungal conidiophore morphology and phylogenetic analysis of the ITS1-5.8S-ITS2 rDNA sequence reveals a close relationship between the enteropathogenic strains Bbm1 and Bbm2 and the non-enteropathogenic strains of *B. bassiana* (Figures 3A and S8B). However, the conidial sizes of Bbm1 (3.73 ± 0.05 μm, n = 30) and Bbm2 (3.57 ± 0.06 μm, n = 30) are significantly larger than those of non-enteropathogenic strains (Bb2390, 2.51 ± 0.03 μm, n = 29; ARSEF252, 2.58 ± 0.03 μm, n = 30) (Figures 3A and 3B). Based on these results, we designated Bbm1 and Bbm2 as a variety of *B. bassiana*, specifically denoted as Bbm.

Conidial germination is the initial step for fungal pathogenesis. Rapid germination may not only enable the fungus to penetrate the cuticle more quickly but may also reduce elimination via food passage during intestinal invasion. A recent study showed a positive correlation between conidial germination speed and fungal virulence.[29] To assess whether the highly virulent strain Bbm1 germinates more rapidly than a less virulent strain, conidial germination rates of Bbm1 and ARSEF252 were determined by topically inoculating silkworm larvae with conidial suspensions, followed by scanning electron microscopy. The results showed that Bbm1 conidia germinated faster than the less virulent strain ARSEF252. Bbm1 conidia began to form germ tubes at 24 h after topical inoculation and developed into long hyphae by 48 h post-infection, whereas ARSEF252 conidia began germinating only at 48 h post-infection (Figure S9A). At approximately 64 h post-inoculation, hyphal bodies of Bbm1 were present in the larval hemolymph, and numerous hyphal bodies were observed at 84 h post-topical inoculation (Figure S9B). In contrast, only a few hyphal bodies of ARSEF252 were observed by 91 h post-infection, and the proliferation of ARSEF252 hyphal bodies was not evident until 112 h after topical inoculation (Figure S9B). Similarly, Bbm1 germinated significantly faster than ARSEF252 when cultured in Sabouraud Dextrose Broth (SDB) liquid medium (Figure S10). These results suggest that rapid germination may be a crucial factor contributing to fungal *per os* virulence.

Bbm exhibits adaptation to high alkalinity

The gut environment in most lepidopteran larvae is highly alkaline, typically ranging from pH 10.0 to 11.5, creating an inhospitable setting for pathogen colonization.[16,30,31] Surprisingly, Bbm1 conidia demonstrated rapid germination in the foregut of silkworm larvae (Figure 2E), indicating resilience to the elevated alkaline pH. To evaluate the impact of high alkalinity on fungal conidial germination, Bbm1, Bbm2, ARSEF252, and Bb2390 conidia were inoculated into SDB liquid medium at various pH levels. At pH 7.0, Bbm1 and Bbm2 conidia began to germinate after 3 and 6 h of incubation, respectively. In contrast, the conidia of ARSEF252 and Bb2390 did not germinate until 9 h after incubation (Figure 3C). Under highly alkaline conditions (pH 11.0), simulating the alkaline foregut environment, Bbm1 and Bbm2 conidia exhibited the most rapid germination rate, which began at 6 h and ended at 15 h after incubation. However, the germination of ARSEF252 and Bb2390 conidia was significantly delayed (from 9 to 24 h) (Figure 3D). The median germination time (GT_{50}) of Bbm1 and Bbm2 conidia was significantly lower than that of ARSEF252 and Bb2390 conidia (Figures 3E and 3F). These results indicate that Bbm strains exhibit rapid responsiveness and a robust tolerance to ambient alkaline pH. This characteristic may aid in their adaptation to the highly alkaline gut lumen of lepidopteran larvae.

BbmPacC activation is required for alkaline tolerance and intestinal infection

The adaptation of fungi to alkaline pH is regulated by the evolutionarily conserved transcription factor PacC, which controls pH-responsive gene expressions.[32] Using PCR and subsequent sequencing with primers designed based on the *PacC* sequence from ARSEF2860 (GenBank: BBA_05984), we identified the

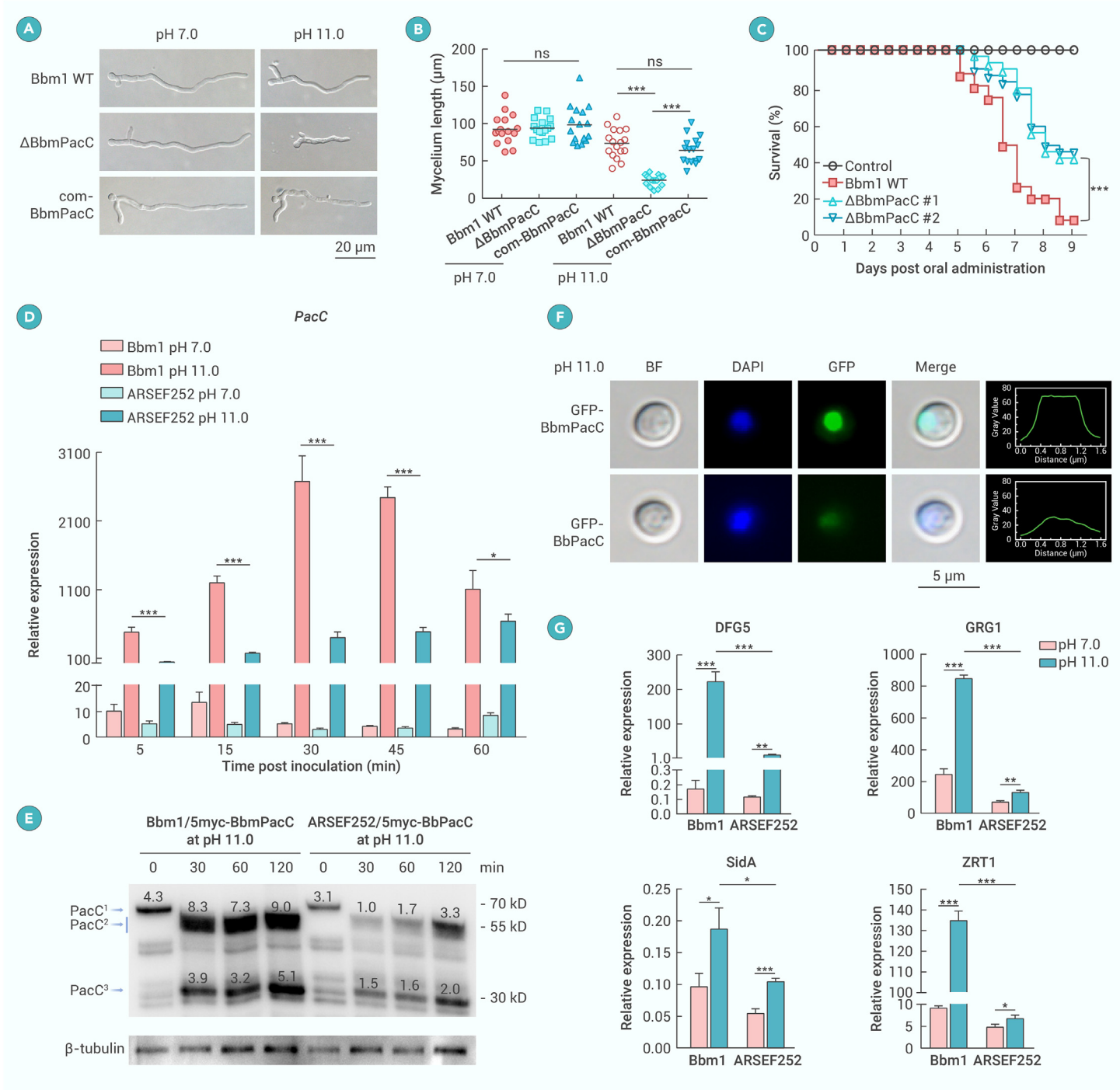

Figure 4. Rapid upregulation and efficient proteolytic processing of BbmPacC contribute to alkaline tolerance and intestinal infection (A and B) Fungal mycelia (A) and their length (B) of Bbm1 WT, ΔBbmPacC, and com-BbmPacC after culture in SDB at pH 7.0 or 11.0 for 15 h. Experiments were performed in three biological replicates. The bars represent the mean. ***$p < 0.001$. (C) Survival rate of silkworm larvae after oral administration of Bbm1 WT and ΔBbmPacC conidia. Experiments were performed in three biological replicates. ***$p < 0.001$. (D) Gene expression of *BbmPacC* and *BbPacC* responses to ambient alkaline pH. *actin* was used as a reference gene. The error bars represent the mean ± SD. ***$p < 0.001$ and *$p < 0.05$. (E) Western blotting analysis of the proteolytic processing of BbmPacC and BbPacC responses to ambient alkaline pH. (F) Micrographs and linescan graph showing subcellular localization of PacC fused with GFP at the N terminus in different strains under alkaline conditions. Conidia of ΔBbmPacC/GFP-BbmPacC and ΔBbPacC/GFP-BbPacC were inoculated in SDB liquid medium with pH 11.0. DAPI stain indicates the nucleus. (G) Expression of PacC target genes in Bbm1 and ARSEF252 in response to ambient alkaline pH. Total RNAs were isolated from Bbm1 and ARSEF252 conidia cultivated in SDB liquid medium at pH 7.0 or 11.0 for 45 min. *actin* was used as a reference gene. The error bars represent the mean ± SD. ***$p < 0.001$, **$p < 0.01$, and *$p < 0.05$.

PacC orthologs in Bbm1 and ARSEF252, denoting them as *BbmPacC* and *BbPacC*, respectively (Figure S11). To determine whether PacC is involved in alkaline tolerance in Bbm1, we generated the deletion mutants of *BbmPacC* (ΔBbmPacC) and the complementary strain com-BbmPacC (Figure S12). Although the loss of *BbmPacC* did not affect the rapid germination of Bbm1 conidia under neutral or alkaline pH (Figure S13), it significantly inhibited mycelial growth under alkaline conditions. Conversely, the complementary strain com-BbmPacC rescued the phenotypic defect (Figures 4A and 4B), indicating that *BbmPacC* contributes to alkaline tolerance in Bbm1. To determine whether PacC-dependent alkaline adaptation is crucial for fungal *per os* virulence, we examined the pathogenicity of ΔBbmPacC. Oral administration revealed a significant decrease in the *per os* virulence of ΔBbmPacC compared to that of Bbm1 wild type (WT; $p < 0.001$) (Figure 4C), indicating that *BbmPacC* is required for intestinal infection by Bbm1.

Given the highly conserved *PacC* gene sequences between Bbm1 and ARSEF252 (98.75% identity) (Figure S11), we further examined potential

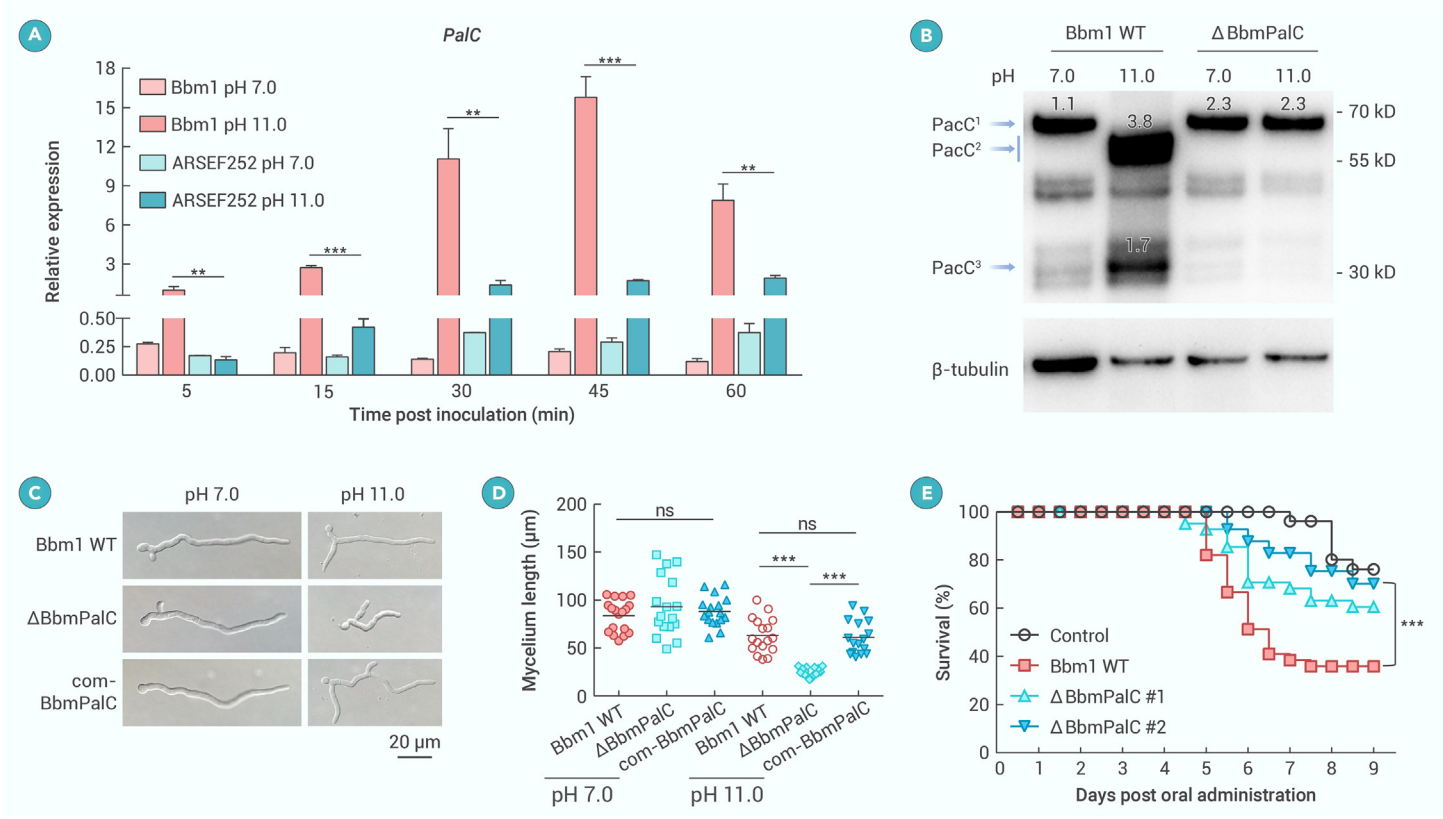

Figure 5. The differentially expressed gene *PalC* is required for transcriptional expression and proteolytic processing of PacC (A) Gene expression of *BbmPalC* and *BbPalC* in responses to ambient alkaline pH. *actin* was used as a reference gene. The error bars represent the mean ± SD. ***$p < 0.001$ and **$p < 0.01$. (B) Western blotting analysis of the proteolytic processing of BbmPacC in Bbm1/5myc-BbmPacC and ΔBbmPalC/5myc-BbmPacC strains in response to ambient alkaline pH. (C and D) Fungal mycelia (C) and their length (D) of Bbm1 WT, ΔBbmPalC, and com-BbmPalC after culture in SDB liquid medium at pH 7.0 or 11.0 for 15 h. Experiments were performed in three biological replicates. The bars represent the mean. ***$p < 0.001$. (E) Survival rate of silkworm larvae after oral administration of Bbm1 WT and ΔBbmPalC conidia. Experiments were performed in three biological replicates. ***$p < 0.001$.

differences in the expression patterns of *BbmPacC* and *BbPacC*. Transcriptional analysis showed that *BbmPacC* transcription level was markedly increased at 5 min after conidia were inoculated in pH 11.0, reaching a peak at 30 min (2,677-fold increase relative to the reference gene *actin*), while *BbPacC* mRNA gradually upregulated during cultivation in pH 11.0 and did not reach the highest expression until 60 min (632-fold increase relative to *actin*) (Figure 4D). These results indicated that the transcription of *BbmPacC* is induced more rapidly than that of *BbPacC* under alkaline conditions.

Under neutral to alkaline conditions, the PacC polypeptide undergoes proteolytic processing by two successive cleavages, resulting in the conversion of the full-length PacC into an intermediate PacC and subsequently into the shortest functional polypeptide.[32,33] To detect the proteolytic processing of BbmPacC and BbPacC under alkaline conditions, we constructed 5myc-BbmPacC fusion and 5myc-BbPacC fusion by inserting a 5×myc tag at the 5′ end of *PacC* in the genomes of Bbm1 and ARSEF252, respectively. Western blotting analysis showed that in Bbm1, $PacC^1$ (the full-length form, ~70 kD) was immediately converted to $PacC^2$ (the intermediate form, ~55 kD) and $PacC^3$ (the active form, ~30 kD) within 30 min under alkaline conditions, and $PacC^3$ accumulated at 120 min (Figure 4E). However, in ARSEF252, $PacC^2$ and $PacC^3$ were much weaker and not obviously detected until 120 min under alkaline conditions, which was significantly slower than those in Bbm1 (Figure 4E). Therefore, PacC cleavage in Bbm1 was significantly more efficient than that in ARSEF252.

After proteolytic cleavages in the cytoplasm, the shortest functional form of PacC is translocated into the nucleus, where it activates the expressions of alkaline-induced genes.[32,33] To observe the subcellular localization of PacC under alkaline conditions, we generated fusion constructs of GFP fused to the N terminus of BbmPacC (GFP-BbmPacC) and BbPacC (GFP-BbPacC) under the control of their respective *PacC* native promoters, which were then transformed into ΔBbmPacC and ΔBbPacC mutant strains, respectively. Under neutral conditions, no obvious GFP signal was observed in the conidia, indicating the low expression of *PacC* at pH 7.0 (Figure S14). After alkaline induction, GFP-BbmPacC was exclusively located in the nucleus of ΔBbmPacC conidia (Figure 4F). However, in ΔBbPacC conidia, the signal of GFP-BbPacC was weak (Figure 4F). Consistent with the proteolytic cleavages and protein localization of PacC, the expressions of PacC binding genes involved in tolerance to alkaline pH, such as DFG5 (defective for filamentous growth 5, a cell-wall glycoprotein), GRG1 (glucose-repressible protein), SidA (L-ornithine N5-monooxygenase), and ZRT1 (zinc/iron transporter protein),[34,35] were highly induced under alkaline condition in Bbm1, significantly higher than those in ARSEF252 (Figure 4G). Taken together, these findings suggest that rapid transcriptional upregulation and efficient proteolytic cleavage of PacC in Bbm1, compared to ARSEF252, can activate the expression of alkaline-induced genes, thus enabling the fungus to adapt to the alkaline intestine of lepidopteran larvae.

PalC plays a crucial role in PacC activation

In fungi, the pH-dependent Pal signaling pathway plays a key role in the proteolytic cleavage of PacC and involves six Pal proteins: PalA, PalB, PalC, PalF, PalH, and PalI.[32] Variations in processing efficiency between BbmPacC and BbPacC suggest potential differences in the actions of upstream Pal proteins between the two strains. To explore this, the transcriptional expression patterns of these six Pal genes were examined in Bbm1 and ARSEF252 under alkaline conditions. The results revealed that only the expression patterns of *PalC* (a homolog of BBA_01909 [GenBank] annotated in *B. bassiana* ARSEF2860 genome) aligned with that of *PacC*, showing significant differences in expression between the two strains (Figures 5A and S15). In Bbm1, *PalC* expression was significantly upregulated after alkaline induction, peaking at 45 min (~15.8-fold to *actin*) (Figure 5A). However, in ARSEF252, *PalC* expression was gradually increased but remained significantly lower than that of Bbm1 under alkaline conditions (Figure 5A). To determine whether *PalC* is essential for PacC activation, *PalC* was deleted in Bbm1 (Figure S12C). At the protein level, neither $PacC^2$ nor $PacC^3$ was detected in ΔBbmPalC under alkaline conditions (Figure 5B),

indicating the blockade of PacC proteolytic cleavage in ΔBbmPalC. Therefore, *PalC* is required for PacC activation at the proteolytic processing level.

Consistent with PacC function, the loss of *PalC* also hindered mycelium growth under alkaline conditions compared to Bbm1 WT, and the complementary strain com-BbmPalC could rescue the phenotypic defect (Figures 5C and 5D). Oral administration of fungal conidia to silkworm larvae showed that *PalC* deletion significantly attenuated the *per os* virulence compared to Bbm1 WT ($p < 0.001$) (Figure 5E), suggesting that *BbmPalC* is also required for intestinal infection by Bbm1. Together, these results highlight the pivotal role of PalC in PacC activation, facilitating fungal adaptation to the alkaline environment of the insect foregut and enabling successful intestinal infection.

Alkaline induction of *PalC* depends on the downstream gene *Aia*

To explore the factors contributing to the differential transcription of *PalC* between Bbm1 and ARSEF252, we scrutinized their promoter and gene body sequences. However, no significant differences were identified between *BbmPalC* and *BbPalC* (Figure S16). Unexpectedly, a 249-bp fragment deletion was identified in the downstream adjacent gene (homolog of BBA_01908 [GenBank] annotated in *B. bassiana* ARSEF2860 genome, predicted to encode hypothetical protein with no conserved domain) of *BbmPalC* of Bbm1 and Bbm2. Notably, this 249-bp fragment was present in the downstream gene of *BbPalC* of non-enteropathogenic strains such as ARSEF252 and ARSEF2860 (Figures 6A, S17, and S18). This downstream adjacent gene with a 249-bp deletion was significantly upregulated in Bbm1 at 45 min after alkaline induction (~4.3-fold increase relative to *actin*), which is consistent with the expression patterns of *BbmPacC* and *BbmPalC* (Figure 6B). However, in ARSEF252, the downstream adjacent gene showed no induction under alkaline conditions (Figure 6B). Hereafter, we designate this gene as *Aia* for the reasons explained below.

To investigate the effect of *BbmAia* on *BbmPalC* transcription, we deleted *BbmAia* in the Bbm1 genome (Figure S12D). Loss of *BbmAia* inhibited the upregulation of *BbmPalC* after alkaline induction compared to that in Bbm1 WT (Figure 6C), indicating that the induction of *BbmPalC* under alkaline conditions relies on *BbmAia*. To determine whether the 249-bp fragment influences the expression of *Aia*, we performed homologous recombination to substitute *BbmAia* with *BbAia*, and vice versa (Figure 6A). The substitution of *BbAia* in Bbm1 (Bbm1/BbAia strain) resulted in significantly lower expression than the native *BbmAia* (Figure 6D), leading to the downregulation of *BbmPalC* and *BbmPacC* after alkaline induction (Figures 6E and 6F). In contrast, the expression of *BbmAia* replaced in ARSEF252 (ARSEF252/BbmAia strain) was significantly higher than the native *BbAia* (Figure 6G), resulting in the upregulation of *BbPalC* and *BbPacC* compared to that in ARSEF252 WT (Figures 6H and 6I). Taken together, these results indicate that the 249-bp fragment hinders the transcription of *PalC* and *PacC*, leading to a slower response of ARSEF252 to alkaline stress. In contrast, the absence of the 249-bp fragment enables *BbmAia* to function as an alkaline inductive activator (hence abbreviated as *Aia*) that significantly boosts the expressions of *PalC* and *PacC*, which helps the fungus tolerate alkaline conditions.

Heterologous expression of BbmPacC^{active} in ARSEF252 facilitates intestinal infection

Due to the inefficient production of the shortest functional form of PacC upon alkaline induction in ARSEF252, we introduced the active form of BbmPacC fused with an myc tag in the N terminus (hereafter referred to as myc-BbmPacC^{active}) in ARSEF252 to improve its alkaline tolerance and ability to cause gut infection (Figures 7A and 7B). The expression of *myc-BbmPacC^{active}* was driven by the native promoter of *BbmPacC* and a predicted nuclear localization sequence in the C terminus of BbmPacC^{active}. Under alkaline conditions, ARSEF252/myc-BbmPacC^{active} exhibited enhanced tolerance to alkaline pH, with longer mycelia than those of ARSEF252 WT (Figures 7C and 7D). Consequently, the expression of myc-BbmPacC^{active} significantly improves the *per os* virulence of ARSEF252, as evidenced by oral administration ($p < 0.001$) (Figure 7E). These results indicate that the active form of BbmPacC promotes fungal alkaline adaptation, thereby facilitating intestinal infection.

DISCUSSION

Entomopathogenic fungi primarily attack insects by penetrating the host integument and proliferating in the hemolymph.[9] The success of fungal pesticides in pest control is heavily influenced by environmental factors. While moist conditions or high RH are typically required for fungal germination and effective insect control, topical fungal infections often exhibit slow-acting killing effects and low control efficiency in the field conditions.[10,11] In this study, we have identified the insect foregut as a previously unrecognized alternative infection route for the fungal pathogen Bbm. Bbm can effectively infect lepidopteran larvae and pupae through the intestinal tract following *per os* inoculation, even at low ambient humidity. Importantly, the dual routes of infection via the external integument and the gut significantly increase the killing speed, providing a strategy for enhancing the potency of fungal insecticides. As shown in Figure 7F, to adapt to the highly alkaline foregut environment of the insect, Bbm1 rapidly upregulates the key transcription factor PacC, which further undergoes efficient proteolytic cleavage to produce the functional form that activates alkaline-induced genes. The activation of PacC requires the highly induced *palC*, a gene in the alkaline-responsive Pal signaling pathway, which is dependent on its adjacent downstream gene *Aia*. In Bbm1 and Bbm2, the loss of a 249-bp fragment in *Aia* leads to highly induced expression under alkaline conditions, promoting the upregulation of *PalC* and enabling PacC activation. This ultimately improves fungal alkaline tolerance, facilitating intestinal infection.

The insect gut consists of three sections based on embryonic origin and physiological function: the foregut, the midgut, and the hindgut. Typically, the foregut is subdivided into a pharynx, an oesophagus (esophagus), and a crop (a food storage area). The foregut and hindgut, which are of ectodermal origin, are lined with a cuticle intima composed of chitin and cuticular glycoproteins, potentially facilitating conidia attachment.[36] The midgut, originating from the embryonic endoderm, lacks a cuticle. The midgut epithelial cells secrete a chitinous peritrophic matrix, which undergoes regular replacement and shedding, along with associated microorganisms. This dynamic process poses a challenge for fungal conidia to germinate or penetrate midgut epithelial cells before being excreted. In contrast, the cuticle lining of the foregut and hindgut is shed along with the exoskeleton only at ecdysis during larval development,[36] providing a relatively stable surface for microbial colonization that may favor fungal invasion. Our histological evidence demonstrates that Bbm1 conidia adhere to the foregut intima, germinate 12 h after *per os* inoculation, penetrate the foregut wall, and enter the hemocoel, ultimately causing insect death. This study reveals the foregut, rather than the midgut or hindgut, as the previously unrecognized site of invasion for fungal pathogens.

Rapid germination has been recognized as an important virulence factor in certain host-pathogen associations.[37] However, in leaf-fed larvae, fungal conidia are rapidly expelled from the intestinal tract. For example, the vast majority of *M. anisopliae* conidia were flushed out of the locust gut before germination occurred.[20] In addition, the rapid passage of food through the gut is considered an important factor preventing gut invasion of *B. bassiana* in the Colorado potato beetle, *Leptinotarsa decemlineata*.[19,20] Therefore, rapid germination in the gut can prevent the extrusion of the fungal inoculum during food passage, thereby increasing the likelihood of fungal infection. In our study, we observed that Bbm strains exhibited faster germination than less virulent strains, particularly in the alkaline conditions, facilitating the rapid establishment of gut colonization and invasion by the fungus.

The lepidopteran larval gut is recognized for its highly alkaline nature, with a pH range of 10.0–11.5 in the foregut and midgut of *B. mori* larvae and approximately 10.0 in the hindgut.[30,31] This extreme alkalinity of the larval gut may contribute to the rare incidence of lepidopteran gut infection by entomopathogenic fungi. High pH has been shown to impede *B. bassiana* germination and prevent fungal colonization of the larval gut in certain species, such as *B. mori* and *Helicoverpa zea*.[16,17] However, our study revealed that the Bbm strains Bbm1 and Bbm2 are only slightly affected by highly alkaline conditions (pH 11.0), indicating that Bbm is resistant to extreme alkaline of the foregut.

Fungi have evolved a conserved Pal signaling pathway in response to ambient alkaline pH, which has been reported in model fungi such as *Saccharomyces cerevisiae* and *Aspergillus nidulans*, as well as fungal pathogens like *Sclerotinia sclerotiorum*, *Penicillium expansum*, and *Fusarium graminearum*.[32,33,38,39] This pathway involves the membrane receptor PalH, which senses the alkaline pH signal and mediates ubiquitination and phosphorylation of PalF, leading to endocytosis of the receptor complex, followed by recruitment of the endosomal sorting complexes required for transport (ESCRT) by PalC, which transmits the signal from the plasma membrane to the endosomal membrane complex on the surface of the endosome.[40] The zinc-finger transcription factor PacC, bound by

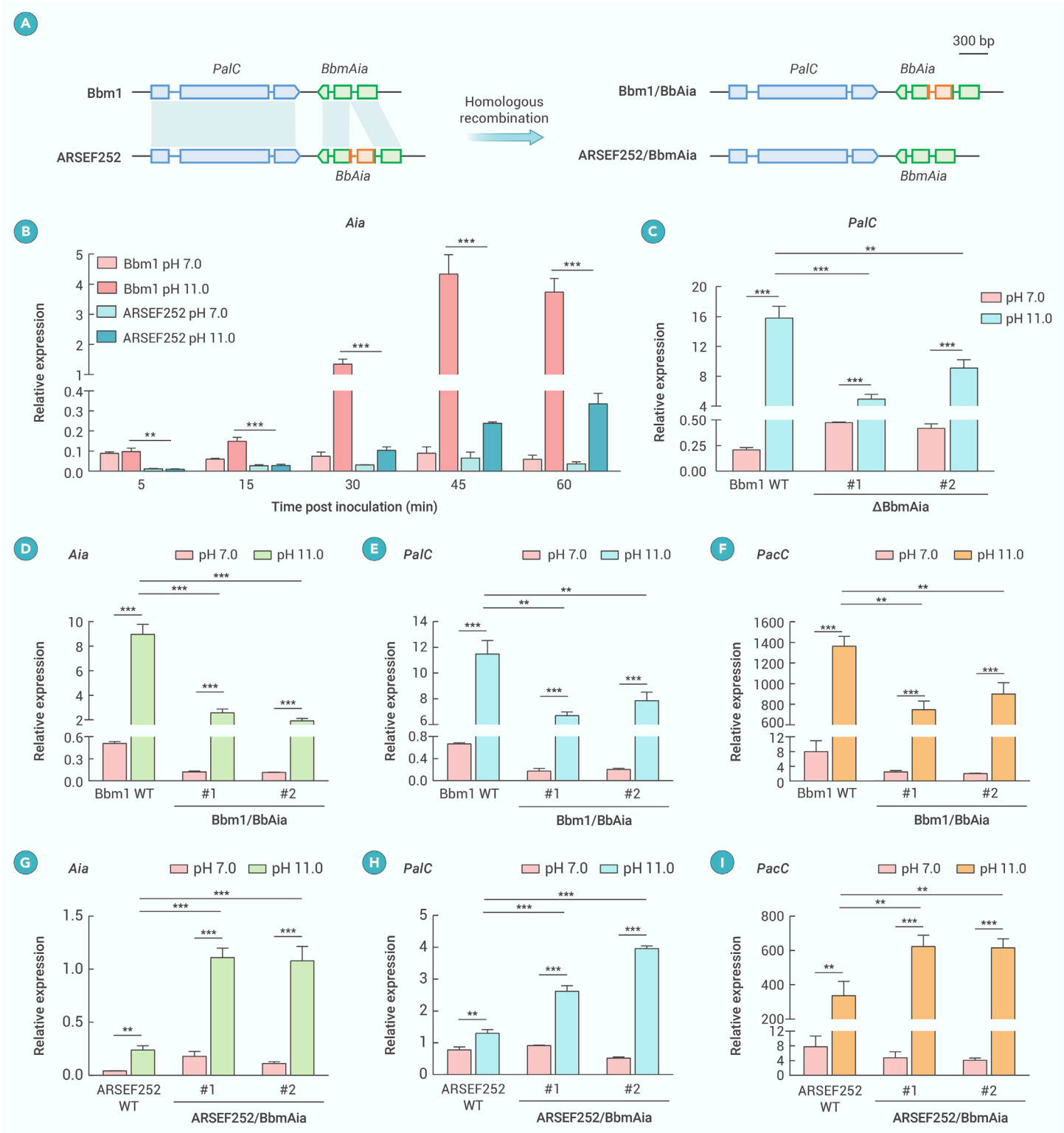

Figure 6. The downstream gene *Aia* promotes *PalC* expression (A) Gene locus alignment of *PalC* and *Aia* in Bbm1 and ARSEF252. Compared to *BbAia*, *BbmAia* does not have a 249-bp fragment. *BbAia* and *BbmAia* were exchanged into Bbm1 and ARSEF252 genomes based on homologous recombination. (B) Gene expression of *BbmAia* and *BbAia* in response to ambient alkaline pH. (C) Expression of *PalC* in Bbm1 and ΔBbmAia in response to ambient alkaline pH. Total RNAs were isolated from Bbm1 and ΔBbmAia conidia cultivated in SDB liquid medium at pH 7.0 or 11.0 for 45 min. (D–F) Expression of *Aia* (D), *PalC* (E), and *PacC* (F) in Bbm1 WT and Bbm1/BbAia recombinant strains in response to ambient alkaline pH. (G–I) Expression of *Aia* (G), *PalC* (H), and *PacC* (I) in ARSEF252 WT and ARSEF252/BbmAia recombinant strains in response to ambient alkaline pH. For (C-I), total RNAs were isolated from fungal conidia cultivated in SDB liquid medium at pH 7.0 or 11.0 for 45 min. For (B-I), *actin* was used as a reference gene. ***$p < 0.001$ and **$p < 0.01$.

PalA, undergoes pH-dependent proteolysis mediated by the cysteine protease PalB. The resulting truncated and functional PacC is then translocated into the nucleus and induces the activation of alkaline-expressed genes and the repression of acid-expressed genes.[32] Additionally, in *B. bassiana*, PacC positively regulates the synthesis of oosporein, a red dibenzoquinone pigment that inhibits dual oxidase expression in the midgut during topical infection and inhibits bacterial growth after host death.[41,42] However, PacC and the six *pal* genes have only minor effect on *B. bassiana* virulence via topical infection against *Galleria mellonella* larvae.[43,44] Surprisingly, our study found that PacC is required for alkaline tolerance of and intestinal infection by Bbm, indicating that PacC functions as

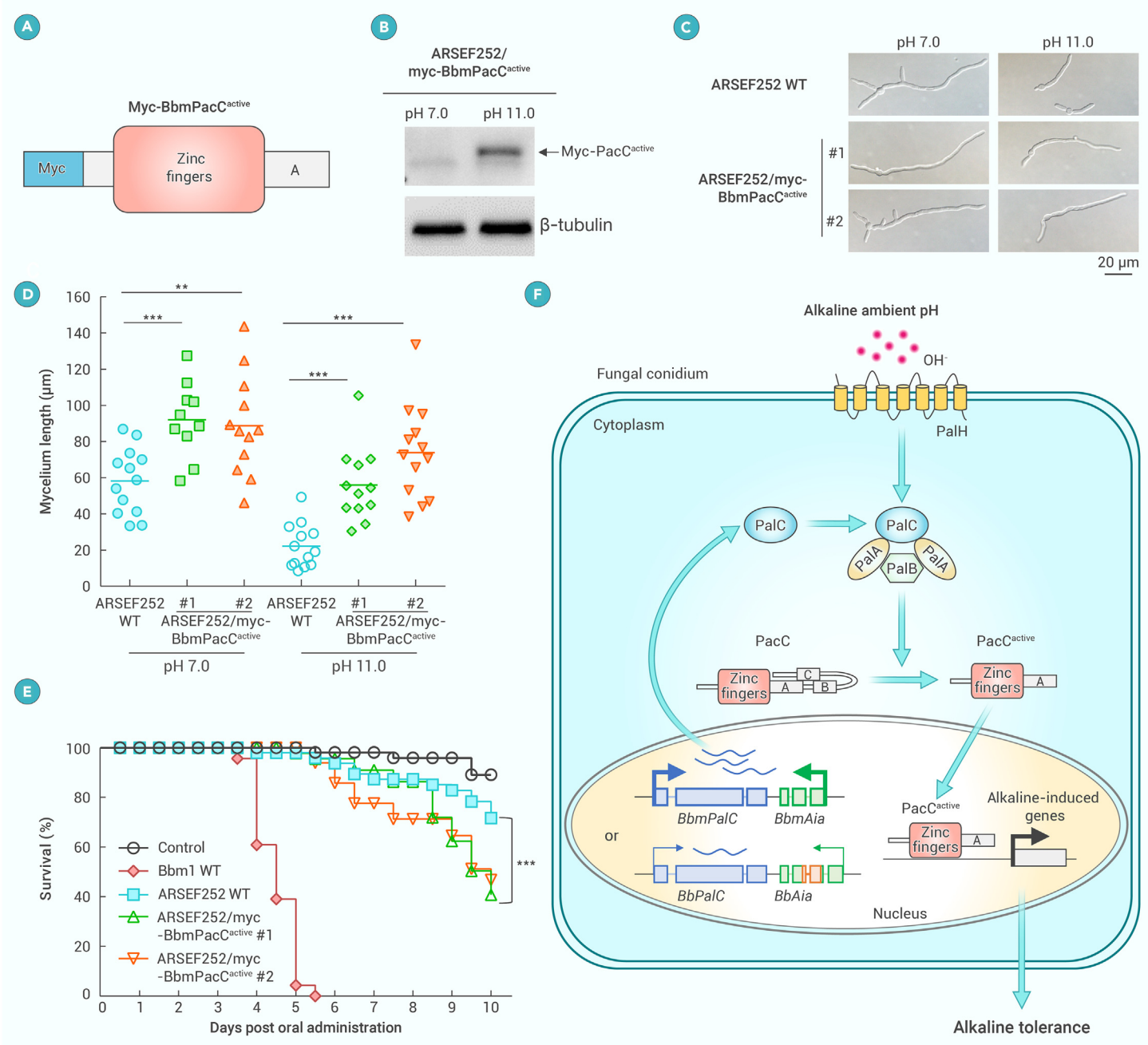

Figure 7. Heterologous expression of the active form of BbmPacC in ARSEF252 facilitates intestinal infection (A) Protein structure of the active form of BbmPacC (Myc-BbmPacC^{active}). (B) Western blotting analysis of Myc-BbmPacC^{active} expression in response to ambient alkaline pH. (C and D) Fungal mycelia (C) and their length (D) of ARSEF252 WT and ARSEF252/myc-BbmPacC^{active} after culture in SDB liquid medium at pH 7.0 or 11.0 for 15 h. Experiments were performed in three biological replicates. The bars represent the mean. ***$p < 0.001$ and **$p < 0.01$. (E) Survival rate of silkworm larvae after oral administration of Bbm1 WT, ARSEF252 WT, and ARSEF252/myc-BbmPacC^{active} conidia. Experiments were performed in three biological replicates. ***$p < 0.001$. (F) A schematic model of a novel pH-responsive Aia-PalC-PacC pathway required for fungal alkaline tolerance and intestinal infection against insects. Bbm, a new variety, is capable of infecting lepidopteran larvae through both the integument and gut. Bbm has evolved alkaline tolerance to adapt to the hostile and highly alkaline foregut. The pH-dependent transcription factor PacC in Bbm undergoes rapid upregulation and efficient proteolytic processing in response to the alkaline pH. Activation of PacC relies on the involvement of the Pal protein PalC. Expression of *PalC* is regulated by its adjacent downstream gene *Aia*. Compared to the non-enteropathogenic virulent strains, *BbmAia* loses a 249-bp fragment and is highly induced under alkaline conditions, leading to its function as an alkaline inductive activator that promotes the upregulation of *PalC*. This in turn facilitates PacC processing and activation, enhancing fungal alkaline tolerance, and enables intestinal infection.

a specific virulence factor for gut infection. Although PacC is conserved among fungi, the responses to alkaline conditions among *Beauveria* strains are different due to the differential expression patterns of PacC. When exposed to an alkaline environment, Bbm1 immediately upregulates PacC, which undergoes efficient proteolytic processing into the active form that allows the strain to adapt to the insect's alkaline foregut. This is also confirmed by the heterologous expression of the truncated active PacC, which can enable intestinal infection by the non-enteropathogenic strain ARSEF252.

Furthermore, we found that the alkaline pH-responsive signaling pathway gene *PalC* is differentially expressed between the enteropathogenic and non-enteropathogenic strains. PalC contains a Bro1 domain that specifically interacts with ESCRT-III, and this binding is essential for pH signaling.[32,40,45] As expected, the highly induced *PalC* plays a pivotal role in PacC activation, leading to the alkaline tolerance of Bbm. However, how *PalC* is upregulated under alkaline conditions and differentially expressed was unknown before. In this study, we discovered that the upregulation of *PalC* depends on its adjacent downstream gene *Aia*. In contrast to non-enteropathogenic virulent strains such as ARSEF252, *Aia* in Bbm undergoes a deletion of a 249-bp fragment, transforming it into an alkaline inductive activator. Consequently, the expression of *Aia* in Bbm is highly induced under alkaline conditions. This induction triggers the upregulation of *PalC*,

facilitating the activation of PacC. This enables the fungus to rapidly respond to the alkaline environment and establish intestinal infection through the insect foregut. However, the relatively lower induction of *palC* and *pacC* observed in the ARSEF252/BbmAia strain at pH 11.0, as compared to the endogenous *palC* and *pacC* genes in Bbm1, implies the presence of additional regulatory mechanisms. Notably, the downstream transcription factor PacC plays a key role in upregulating alkaline-induced genes to enhance alkaline tolerance. Therefore, instead of deleting the 249-bp fragment in a non-enteropathogenic Bb strain, heterologous expression of the active form of BbmPacC in ARSEF252 is anticipated to be a more effective way to facilitate intestinal infection. Moreover, similar to topical infection, intestinal infection involves a complex process that requires multiple strategies. The fact that the *per os* virulence of the mutant ΔBbmPacC is not completely abolished indicates that, apart from alkaline tolerance, other factors such as adhesion, intestinal wall degradation, and the production of toxins may also play a role in gut infection, which are exciting future directions.[46]

CONCLUSION

Our study reveals the insect foregut as an alternative and previously unrecognized route for fungal invasion and highlights the rapid infectivity of Bbm in lepidopteran larvae through *per os* infection, even under conditions of low ambient humidity. The dual routes of infection, via integument and gut, significantly accelerate the speed of larval mortality. This not only enhances the efficacy of fungal insecticides but also paves the way for a highly promising strategy in effectively managing lepidopteran pests. We found that Bbm has evolved alkaline tolerance through the novel pH-responsive Aia-PalC-PacC pathway to adapt to the alkaline gut environment, facilitating successful intestinal infection. These findings advance our understanding of fungal pathogenesis in insects, provide novel insights into fungal adaptation to highly alkaline conditions and gut environment of lepidopteran larvae, and lay the foundation for the development of a new generation of fungal insecticides and for designing novel strategies for the management of destructive insect pests.

MATERIALS AND METHODS

Fungal strains and culture

Fifteen *B. bassiana* strains were used in this study (Table S1). The strains ARSEF252 and ARSEF2860 were obtained from the USDA/ARS Collection of Entomopathogenic Fungal Cultures (Ithaca, NY, USA). The strain BbHNG was obtained from Sericultural Research Institute, Chinese Academy of Agricultural Sciences. Others fungal strains were obtained from the Research Center of Entomopathogenic Fungi collection, Anhui Agricultural University (Hefei, China). The fungi were maintained on Sabouraud's dextrose agar plus 1% yeast extract (SDAY). The conidia used for bioassays were harvested from 12-day-old cultures on SDAY agar plates.

Insects and rearing

We used two lepidopteran insects (the silkworm *B. mori* and the soybean pest *C. bilineata*). Larvae of the silkworm *B. mori* were reared on fresh mulberry leaves at 25°C ± 1°C and 75% ± 5% RH under a photoperiod of 14-h/10-h light/dark in a constant temperature and humidity incubator (BSC-250, BoXun China). Larvae of *C. bilineata* were reared on fresh soybean leaves at 25°C ± 1°C and 75% ± 5% RH with a photoperiod of 12-h/12-h light/dark in a constant temperature and humidity incubator.

Elimination of the gut bacteria of *B. mori*

To remove the gut bacteria of silkworm, the larvae were fed on fresh mulberry leaves that had been sprayed with antibiotics (25 μg/mL gentamicin, 10 μg/mL penicillin, 10 units/mL streptomycin = 1:1:1) from the first day of the third-instar stage until they were fed mulberry leaves that had been dipped in conidial suspension (2×10^7 conidia/mL) followed by air drying. The normally reared larvae were fed fresh mulberry leaves without antibiotics.

Fungal infection

For topical inoculation, the silkworm larvae were sprayed with a suspension of 5×10^7 conidia/mL using a 1-mL glass atomizer. Topically inoculated larvae were reared on fresh mulberry leaves at 26°C under a photoperiod of 14-h/10-h light/dark and maintained at high RH (>96% RH) during the first 2 days after topical inoculation and then kept at 80% ± 5% RH in a constant temperature and humidity incubator.

For *per os* bioassays, the silkworm larvae were either fed for 24 h on fresh mulberry leaves that had been dipped in a suspension of 2×10^7 conidia/mL followed by air drying or *per os* inoculated by orally feeding with 1 μL of a suspension 1×10^8 conidia/mL (10^5 conidia/larva) using a 2-μL micropipette. Then, the larvae were immediately surface sterilized with 70% ethanol using cotton wool after oral administration of the conidial suspension. In addition, the *per-os*-inoculated larvae were reared at 26°C under a photoperiod of 14-h/10-h light/dark in constant low ambient humidity (35% ± 5% RH) in a constant temperature and humidity incubator to prevent cuticular infection by the potentially contaminated conidia attaching to cuticle surfaces. The larvae were supplied daily with fresh mulberry leaves.

C. bilineata larvae were orally fed with 1 μL Bbm1 conidia suspension (1×10^8 conidia/mL) using a 2-μL micropipette. The *per-os*-inoculated larvae were reared at 26°C with a photoperiod of 12-h/12-h light/dark in constant low ambient humidity (35% ± 5% RH) and supplied daily with fresh soybean leaves.

Control insects were treated with 0.01% Triton X-100. Mortality was recorded at 12-h intervals. Each treatment was replicated three times with 30–50 insects per replicate, and the bioassays were repeated three times. Dead insects were surface sterilized in 1% bleach for 3 min, rinsed once in 70% ethanol and three times in sterile distilled water, placed on sterile Petri dishes containing wet cotton, and incubated at 25°C to encourage fungal emergence.

Phylogenetic analysis

Full-length sequences of the internal transcribed spacer region of rDNA (ITS1-5.8S rRNA-ITS2) were amplified using universal Primers ITS1 (5′-TCCGTAGGTGAACCTGCGG-3′) and ITS4 (5′-TCCTCCGCTTATTGATATGC-3′) as described by White et al.[47] The PCR products were purified and sequenced. The resulting sequences were aligned with sequences in the GenBank database. A phylogenetic tree was constructed by using the neighbor-joining method, which involved sequence alignments, distance calculations, and cluster analysis with ClustalW and MEGA7.0 software packages.[48] Phylogenetic and molecular evolutionary analysis was inferred by using the neighbor-joining method.[49]

Histologic imaging

The dissected silkworm larval guts were collected into the fixative solution (absolute alcohol/chloroform/glacial acetic acid = 6:3:1 by volume) for 48 h as previously described.[50] The fixed tissues were washed in 70% ethanol twice and dehydrated in 100% ethanol three times (1 h for each). Alcohol was then removed with xylene three times (15 min for each). The tissues were then impregnated and embedded in paraffin wax (P3683, Sigma) for 2 h. Finally, paraffin sections of 5 μm were cut on a microtome (RM2235, Leika) and stained with periodic acid-Schiff (G1285, Solarbio) for microscope investigation.[51]

Scanning electron microscopy

The specimens were fixed in formalin/acetic acid/alcohol solution (formalin/acetic acid/50% alcohol = 1:1:18 by volume) for 24 h and dehydrated in a graded ethanol series (70%, 80%, and 90% ethanol and two 100% ethanol steps) with 20 min at each step. The specimens were then dehydrated in a critical point dryer with liquid CO_2. The dehydrated specimens were coated with gold-palladium and observed in a scanning electron microscope (JSM-6360LV, JEOL).

Fungal germination analysis

25 μL of a conidia suspension (5×10^7 conidia/mL) was inoculated into 5.5-cm polystyrene Petri dishes containing 3 mL SDB with different pH (7.0 and 11.0) and incubated at 27°C. The germination rate was recorded every 3 h. Each treatment was replicated three times, and the assays were repeated twice.

Construction of *B. bassiana* gene deletion and expression strains

For targeted deletion of the *BbmPacC*, *BbPacC*, *BbmPalC*, and *BbmAia* genes separately, the 5′ and 3′ flanking regions of each open reading frame were PCR amplified from the Bbm1 and ARSEF252 genomic DNA as a template, respectively, and then subcloned into the *Xba*I and *Eco*RV sites of the binary vector pBarGFP, respectively. The gene disruption constructs were then used to separately transform *Agrobacterium tumefaciens* AGL-1 for targeted gene disruption by split-marker homologous recombination. Replacement-specific PCR amplifications of the gene locus were performed using specific primer pairs (Table S2) to amplify either the WT or mutated gene locus.[52]

To tag PacC with 5×myc *in situ*, the strains Bbm1/5myc-BbmPacC and ARSEF252/5myc-BbPacC were constructed by inserting a sequence encoding a 5×myc tag at the native genomic locus of the *PacC* gene in Bbm1 and ARSEF252, respectively. The native promoter and the coding region of *PacC* with a 5×myc tag sequence after the start codon ATG were PCR amplified and subcloned into the *Xba*I and *Eco*RV sites of the binary vector pSurGFP to generate plasmids pSurGFP-5myc-BbmPacC and pSurGFP-5myc-BbPacC, respectively. AGL-1 cells containing the respective plasmid were then transformed into

Bbm1 and ARSEF252, respectively, to generate 5myc-BbmPacC and 5myc-BbPacC fusion *in situ*, using the split-marker homologous recombination via *A. tumefaciens*-mediated transformation.

To express GFP-PacC, the native promoter, the coding region of *PacC* with a GFP sequence after the start codon ATG, and its native terminator were PCR amplified and subcloned into the *Eco*RV and *Xho*I sites of the binary vector pSur (delete GFP from pSurGFP) to generate the plasmids pSur-GFP-BbmPacC and pSur-GFP-BbPacC, respectively. AGL-1 cells containing the respective plasmid were then transformed into ΔBbmPacC and ΔBbPacC via *A. tumefaciens*-mediated transformation to generate the strains ΔBbmPacC/GFP-BbmPacC and ΔBbPacC/GFP-BbPacC, respectively.

To heterologously express myc-BbmPacC^{active} in ARSEF252, the native promoter, the truncated coding region of *BbmPacC* with a myc tag sequence after the start codon ATG, and its native terminator were PCR amplified and subcloned into the *Eco*RV site of the binary vector pSurGFP to generate the plasmid pSurGFP-myc-BbmPacC^{active}. AGL-1 cells containing the plasmid were then transformed into ARSEF252 via *A. tumefaciens*-mediated transformation to generate the strain ARSEF252/myc-BbmPacC^{active}.

To replace *BbmAia* in Bbm1 with *BbAia*, the 5′ and 3′ flanking regions of *BbmAia* were PCR amplified from the Bbm1 genomic DNA as a template and then subcloned into the *Xba*I and *Eco*RV sites of the binary vector pSurGFP, respectively. The coding region of *BbAia* and its native promoter and terminator were PCR amplified from the ARSEF252 genomic DNA as a template and subcloned into the *Xba*I site of the binary vector pSurGFP. AGL-1 cells containing the generated plasmid pSurGFP-BbAia was then transformed into ΔBbmAia via *A. tumefaciens*-mediated transformation to generate the strain Bbm1/BbAia. Likewise, ARSEF252/BbmAia was constructed to replace *BbAia* in ARSEF252 with *BbmAia*.

RNA isolation and RT-qPCR

To monitor the transcription of target genes, fungal conidia incubated in SDB (pH 7.0 or 11.0) at 27°C and 200 rpm for 5, 15, 30, 45, and 60 min were collected via centrifugation, lyophilized, and ground in liquid nitrogen. Total RNA was extracted using an RNAiso Plus Kit (Takara D9108A), and cDNA was synthesized using the PrimeScript RT Reagent Kit with gDNA Eraser (Takara DRR047A) according to the manufacturer's instructions. Then, qPCR was performed using a Hieff qPCR SYBR Green Master Mix Kit (Yeason 11201ES08) and a PikoReal instrument (Thermo N11471) under the following conditions: denaturation at 95°C for 5 min, followed by 40 cycles of denaturation at 95°C for 10 s and annealing and extension at 60°C for 30 s. The primers used for the target genes and the reference gene *actin* are listed in Table S2.

Protein extraction and western blotting analysis

Fungal conidia were cultivated at 27°C and 200 rpm in SDB liquid medium at pH 7.0 for 4 h or at pH 11.0 for 30, 60, and 120 min. They were next harvested by centrifugation, lyophilized, and ground in liquid nitrogen. Total proteins were extracted using RIPA lysis buffer (Beyotime) with 1 × protease inhibitor cocktail (Beyotime). Approximately 10–20 μg of total protein per lane was separated by sodium dodecyl sulfate-polyacrylamide gel electrophoresis. Proteins were then transferred to a PVDF membrane (Bio-Rad) and blotted using standard procedures. Primary antibodies were an myc tag (Abmart, M20002S) and β-tubulin (Abmart, M20005S). The secondary antibody was peroxidase-conjugated AffiniPure goat anti-mouse immunoglobulin G (Jackson ImmunoResearch, 115-035-003).

Statistical analysis

The statistical significance of the survival data was analyzed using a log-rank (Mantel-Cox) test. Other statistical significance was calculated using Student's t test for unpaired comparisons between two treatments. A value of $p < 0.05$ was considered to be statistically significant. All statistics were performed using GraphPad Prism v.5.01 for Windows (GraphPad Software).

DATA AND CODE AVAILABILITY

All data are available in the main text or the supplemental information. Further information and requests for resources and reagents should be directed to and will be fulfilled by the lead contact, Sibao Wang (sbwang@cemps.ac.cn), with a completed materials transfer agreement.

REFERENCES

1. Hajek, A.E. (1997). Ecology of terrestrial fungal entomopathogens. In Advances in Microbial Ecology, J.G. Jones, ed. (Plenum Press Div Plenum Publishing Corp), pp. 193–249. https://doi.org/10.1007/978-1-4757-9074-0-5.
2. Wang, S.B., O'Brien, T.R., Pava-Ripoll, M., et al. (2011). Local adaptation of an introduced transgenic insect fungal pathogen due to new beneficial mutations. Proc. Natl. Acad. Sci. USA ***108***(51): 20449–20454. https://doi.org/10.1073/pnas.1113824108.
3. Blanford, S., Chan, B.H.K., Jenkins, N., et al. (2005). Fungal pathogen reduces potential for malaria transmission. Science ***308***(5728): 1638–1641. https://doi.org/10.1126/science.1108423.
4. Knols, B.G.J., Bukhari, T., and Farenhorst, M. (2010). Entomopathogenic fungi as the next-generation control agents against malaria mosquitoes. Future Microbiol. ***5***(3): 339–341. https://doi.org/10.2217/fmb.10.11.
5. Wang, C.S., and Wang, S.B. (2017). Insect pathogenic fungi: Genomics, molecular interactions, and genetic improvements. Annu Rev. Entomol. ***62***: 73–90. https://doi.org/10.1146/annurev-ento-031616-035509.
6. Jiang, L., Goldsmith, M.R., and Xia, Q. (2021). Advances in the arms race between silkworm and baculovirus. Front. Immunol. ***12***: 628151. https://doi.org/10.3389/fimmu.2021.628151.
7. Vertyporokh, L., Hulas-Stasiak, M., and Wojda, I. (2020). Host-pathogen interaction after infection of *Galleria mellonella* with the filamentous fungus *Beauveria bassiana*. Insect Sci. ***27***(5): 1079–1089. https://doi.org/10.1111/1744-7917.12706.
8. Zhang, Y.H., and Ju, F. (2023). Fighting caterpillar pests and managing agricultural insecticide resistance with Lepidoptera-associated *Enterococcus casseliflavus*. Innovation Life ***1***(3): 100042. https://doi.org/10.59717/j.xinn-life.2023.100042.
9. Vega, F.E., Meyling, N.V., Luangsa-Ard, J.J., et al. (2012). Fungal entomopathogens. In Insect Pathology, F.E. Vega and H.K. Kaya, eds. (Academic Press), pp. 171–220. https://doi.org/10.1016/B978-0-12-384984-7.00006-3.
10. Jaronski, S.T. (2010). Ecological factors in the inundative use of fungal entomopathogens. BioControl ***55***(1): 159–185. https://doi.org/10.1007/s10526-009-9248-3.
11. Lacey, L.A., Frutos, R., Kaya, H.K., et al. (2001). Insect pathogens as biological control agents: Do they have a future? Biol. Control ***21***(3): 230–248. https://doi.org/10.1006/bcon.2001.0938.
12. Lopes, R.B., Martins, I., Souza, D.A., et al. (2013). Influence of some parameters on the germination assessment of mycopesticides. J. Invertebr. Pathol. ***112***(3): 236–242. https://doi.org/10.1016/j.jip.2012.12.010.
13. Mishra, S., Kumar, P., and Malik, A. (2015). Effect of temperature and humidity on pathogenicity of native *Beauveria bassiana* isolate against *Musca domestica* L. J. Parasit. Dis. ***39***(4): 697–704. https://doi.org/10.1007/s12639-013-0408-0.
14. Mannino, M.C., Huarte-Bonnet, C., Davyt-Colo, B., et al. (2019). Is the insect cuticle the only entry gate for fungal infection? Insights into alternative modes of action of entomopathogenic fungi. J. Fungi ***5***(2): 33. https://doi.org/10.3390/jof5020033.
15. Charnley, A.K. (1984). Physiological aspects of destructive pathogenesis in insects by fungi: a speculative review. In Invertebrate-Microbial Interactions (Cambridge University Press), pp. 229–270.
16. Gabriel, B. (1959). Fungus infection of insects via the alimentary tract. J Insect Pathol ***1***: 319–330.
17. Pekrul, S., and Grula, E.A. (1979). Mode of infection of the corn earworm (*Heliothis zea*) by *Beauveria bassiana* as revealed by scanning electron microscopy. J. Invertebr. Pathol. ***34***(3): 238–247. https://doi.org/10.1016/0022-2011(79)90069-7.
18. Dillon, R.J., and Charnley, A.K. (1988). Inhibition of *Metarhizium anisopliae* by the gut bacterial flora of the desert locust: characterisation of antifungal toxins. Can J. Microbiol. ***34***(9): 1075–1082. https://doi.org/10.1139/m88-189.
19. Allee, L.L., Goettel, M.S., Gol'berg, A., et al. (1990). Infection by *Beauveria bassiana* of *Leptinotarsa decemlineata* larvae as a consequence of fecal contamination of the integument following *per os* inoculation. Mycopathologia ***111***: 17–24. https://doi.org/10.1007/BF02277296.
20. Dillon, R.J., and Charnley, A.K. (1986). Invasion of the pathogenic fungus *Metarhizium anisopliae* through the guts of germfree desert locusts, *Schistocerca gregaria*. Mycopathologia ***96***: 59–66. https://doi.org/10.1007/bf00467687.
21. Schabel, H.G. (1976). Oral infection of *Hylobius pales* by *Metarrhizium anisopliae*. J. Invertebr. Pathol. ***27***(3): 377–383. https://doi.org/10.1016/0022-2011(76)90100-2.
22. Veen, K.H. (1966). Oral infection of second-instar nymphs of *Schistocerca gregaria* by *Metarhizium anisopliae*. J. Invertebr. Pathol. ***8***(2): 254–256. https://doi.org/10.1016/0022-2011(66)90138-8.
23. Dillon, R.J., and Charnley, A.K. (1986). Inhibition of *Metarhizium anisopliae* by the gut bacterial flora of the desert locust, *Schistocerca gregaria*: Evidence for an antifungal toxin. J. Invertebr. Pathol. ***47***(3): 350–360. https://doi.org/10.1016/0022-2011(86)90106-0.
24. Xia, Q.Y., Guo, Y.R., Zhang, Z., et al. (2009). Complete resequencing of 40 genomes reveals domestication events and genes in silkworm (*Bombyx*). Science ***326***(5951): 433–436. https://doi.org/10.1126/science.1176620.
25. Lazzarini, G.M.J., Rocha, L.F.N., and Luz, C. (2006). Impact of moisture on *in vitro* germination of *Metarhizium anisopliae* and *Beauveria bassiana* and their activity on *Triatoma infestans*. Mycol. Res. ***110***: 485–492. https://doi.org/10.1016/j.mycres.2005.12.001.
26. Shapiro-Ilan, D.I., and Mizell, R.F. (2015). An insect pupal cell with antimicrobial properties that suppress an entomopathogenic fungus. J Invertebr Pathol ***124***: 114–116. https://doi.org/10.1016/j.jip.2014.12.003.
27. Ugine, T.A., Wraight, S.P., Brownbridge, M., et al. (2005). Development of a novel bioassay for estimation of median lethal concentrations (LC_{50}) and doses (LD_{50}) of the entomopathogenic fungus *Beauveria bassiana*, against western flower thrips, *Frankliniella occidentalis*. J. Invertebr. Pathol. ***89***(3): 210–218. https://doi.org/10.1016/j.jip.2005.05.010.
28. Vandenberg, J.D., Ramos, M., and Altre, J.A. (1998). Dose-response and age- and temperature-related susceptibility of the diamondback moth (Lepidoptera: Plutellidae) to two isolates of *Beauveria bassiana* (Hyphomycetes: Moniliaceae). Environ. Entomol. ***27***(4): 1017–1021. https://doi.org/10.1093/ee/27.4.1017.

29. Rangel, D.E.N., Braga, G.U.L., Fernandes, E.K.K., et al. (2015). Stress tolerance and virulence of insect-pathogenic fungi are determined by environmental conditions during conidial formation. Curr. Genet. ***61***(3): 383–404. https://doi.org/10.1007/s00294-015-0477-y.
30. Liu, H., Chen, B.S., Hu, S.R., et al. (2016). Quantitative proteomic analysis of germination of *Nosema bombycis* spores under extremely alkaline conditions. Front. Microbiol. ***7***: 1459. https://doi.org/10.3389/fmicb.2016.01459.
31. Ponnuvel, K.M., Kumar, V., Babu, A.M., et al. (1999). Effect of alkalinity and protease in the digestive juice of silkworm, *Bombyx mori* on BmNPV infection. Ital. J. Zool. ***66***(2): 121–124. https://doi.org/10.1080/11250009909356246.
32. Penalva, M.A., Tilburn, J., Bignell, E., et al. (2008). Ambient pH gene regulation in fungi: making connections. Trends Microbiol. ***16***(6): 291–300. https://doi.org/10.1016/j.tim.2008.03.006.
33. Chen, Y., Li, B.Q., Xu, X.D., et al. (2018). The pH-responsive PacC transcription factor plays pivotal roles in virulence and patulin biosynthesis in *Penicillium expansum*. Environ. Microbiol. ***20***(11): 4063–4078. https://doi.org/10.1111/1462-2920.14453.
34. Nobile, C.J., Solis, N., Myers, C.L., et al. (2008). *Candida albicans* transcription factor Rim101 mediates pathogenic interactions through cell wall functions. Cell Microbiol. ***10***(11): 2180–2196. https://doi.org/10.1111/j.1462-5822.2008.01198.x.
35. Trushina, N., Levin, M., Mukherjee, P.K., et al. (2013). PacC and pH-dependent transcriptome of the mycotrophic fungus *Trichoderma virens*. BMC Genomics ***14***: 138. https://doi.org/10.1186/1471-2164-14-138.
36. Nowotschin, S., Hadjantonakis, A.K., and Campbell, K. (2019). The endoderm: a divergent cell lineage with many commonalities. Development ***146***(11): dev150920. https://doi.org/10.1242/dev.150920.
37. Faria, M., Lopes, R.B., Souza, D.A., et al. (2015). Conidial vigor vs. viability as predictors of virulence of entomopathogenic fungi. J. Invertebr. Pathol. ***125***: 68–72. https://doi.org/10.1016/j.jip.2014.12.012.
38. Gu, Q., Wang, Y.J., Zhao, X.Z., et al. (2022). Inhibition of histone acetyltransferase GCN5 by a transcription factor FgPacC controls fungal adaption to host-derived iron stress. Nucleic Acids Res. ***50***(11): 6190–6210. https://doi.org/10.1093/nar/gkac498.
39. Rollins, J.A. (2003). The *Sclerotinia sclerotiorum pac1* gene is required for sclerotial development and virulence. Mol. Plant Microbe ***16***(9): 785–795. https://doi.org/10.1094/mpmi.2003.16.9.785.
40. Penalva, M.A., Lucena-Agell, D., and Arst, H.N. (2014). *Liaison alcaline*: Pals entice non-endosomal ESCRTs to the plasma membrane for pH signaling. Curr. Opin. Microbiol. ***22***: 49–59. https://doi.org/10.1016/j.mib.2014.09.005.
41. Chen, X., Zhang, W.W., Wang, J.Y., et al. (2022). Transcription factors BbPacC and Bbmsn2 jointly regulate oosporein production in *Beauveria bassiana*. Microbiol. Spectr. ***10***(6): e0311822. https://doi.org/10.1128/spectrum.03118-22.
42. Wei, G., Lai, Y.L., Wang, G.D., et al. (2017). Insect pathogenic fungus interacts with the gut microbiota to accelerate mosquito mortality. Proc. Natl. Acad. Sci. USA ***114***(23): 5994–5999. https://doi.org/10.1073/pnas.1703546114.
43. Luo, Z.B., Ren, H., Mousa, J.J., et al. (2017). The PacC transcription factor regulates secondary metabolite production and stress response, but has only minor effects on virulence in the insect pathogenic fungus *Beauveria bassiana*. Environ. Microbiol. ***19***(2): 788–802. https://doi.org/10.1111/1462-2920.13648.
44. Zhu, J., Ying, S.H., and Feng, M.G. (2016). The Pal pathway required for ambient pH adaptation regulates growth, conidiation, and osmotolerance of *Beauveria bassiana* in a pH-dependent manner. Appl. Microbiol. Biot. ***100***(10): 4423–4433. https://doi.org/10.1007/s00253-016-7282-5.
45. Galindo, A., Hervás-Aguilar, A., Rodríguez-Galán, O., et al. (2007). PalC, one of two Bro1 domain proteins in the fungal pH signalling pathway, localizes to cortical structures and binds Vps32. Traffic ***8***(10): 1346–1364. https://doi.org/10.1111/j.1600-0854.2007.00620.x.
46. Aktories, K. (2022). Another surprise in receptor binding of *C. difficile* toxins. Innovation ***3***(4): 100261. https://doi.org/10.1016/j.xinn.2022.100261.
47. White, T.J., Bruns, T., Lee, S., et al. (1990). Amplification and direct sequencing of fungal ribosomal RNA genes for phylogenetics. In A Guide to Molecular Methods and Applications, M.A. Innis, D.H. Gelfand, J.J. Snisky, and T.J. White, eds. (Academic Press), pp. 315–322.
48. Kumar, S., Stecher, G., and Tamura, K. (2016). MEGA7: Molecular Evolutionary Genetics Analysis Version 7.0 for bigger datasets. Mol. Biol. Evol. ***33***(7): 1870–1874. https://doi.org/10.1093/molbev/msw054.
49. Tamura, K., and Nei, M. (1993). Estimation of the number of nucleotide substitutions in the control region of mitochondrial DNA in humans and chimpanzees. Mol. Biol. Evol. ***10***(3): 512–526. https://doi.org/10.1093/oxfordjournals.molbev.a040023.
50. Puchtler, H., Waldrop, F.S., Conner, H.M., et al. (1968). Carnoy fixation: Practical and theoretical considerations. Histochemie ***16***(4): 361–371. https://doi.org/10.1007/BF00306359.
51. Mowry, R.W. (1963). The special value of methods that colour both acidic and vicinal hydroxyl groups in the histochemical study of mucins. With revised directions for the colloidal iron stain, the use of Alcian Blue G8X and their combinations with the periodic acid-schiff reaction. Ann. N.Y. Acad. Sci. ***106***(2): 402–423. https://doi.org/10.1111/j.1749-6632.1963.tb16654.x.
52. Wang, S.B., Fang, W.G., Wang, C.S., et al. (2011). Insertion of an esterase gene into a specific locust pathogen (*Metarhizium acridum*) enables it to infect caterpillars. PLoS Pathog. ***7***(6): e1002097. https://doi.org/10.1371/journal.ppat.1002097.

ACKNOWLEDGMENTS

This work was funded by the National Natural Science Foundation of China (grant nos. 32021001, 32230015, and 32272622), the National Key R&D Program of China (grant no. 2023YFA1801000), the New Cornerstone Science Foundation, Chinese Academy of Sciences (317GJHZ2022028GC), and Youth Innovation Promotion Association CAS (grant no. 2021272). The authors gratefully acknowledge the support of the SANOFI Scholarship Program. We thank Prof. Raymond St. Leger and Dr. Brian Lovett from the University of Maryland and Prof. Marcelo Jacobs-Lorena from the Johns Hopkins University School of Public Health for their comments and suggestions on the manuscript. We also thank Prof. Bo Huang and Prof. Zengzhi Li at Anhui Agricultural University for kindly providing some fungal strains.

AUTHOR CONTRIBUTIONS

S.W. conceived the study. S.W. and Y.L. designed the experiments. Y.L., W.Z., Y.Z., H.L., S.Q., and L.W. performed the experiments. Y.L., W.Z., Y.Z., and S.W. analyzed the data. M.L. contributed new reagents. Y.L. and S.W. wrote the paper.

DECLARATION OF INTERESTS

The authors declare no competing interests.

SUPPLEMENTAL INFORMATION

It can be found online at https://doi.org/10.1016/j.xinn.2024.100644.

LEAD CONTACT WEBSITE

http://www.cemps.cas.cn/yjdy/kcfyyjhswx/kcktz/201812/t20181214_5212383.html.